



Theoretical view on interaction between boron nitride nanostructures and some drugs

Soma Majedi ^{a, *}, Farnaz Behmagham ^b Mahshad Vakili ^c

^a College of Health Sciences, University of Human Development, Sulaimaniyah, Kurdistan region of Iraq

^b Department of Chemistry, Miyandoab Branch, Islamic Azad University, Miyandoab, Iran

^c Department of Chemistry, Miyaneh Branch, Islamic Azad University, Miyaneh, Iran

ARTICLE INFO

ABSTRACT

Article history:

Received 10 April 2020

Received in revised form 21 May 2020

Accepted 2 June 2020

Available online 2 June 2020

Keywords:

Drug delivery
Boron nitride
Nanostructures
DFT

Many advancing aspects of technology and science are in the field of nanotechnology, in which levels and interfaces are of particular importance in determining the performance and usage. One related application in which interactions play an important role is the synthesis of drugs. Nanotechnology and nanodelivery are comparatively modern procedure and rapidly evolving science that uses nanoscale materials to be used as diagnostic systems or delivery of therapeutic drugs to particular aimed address in a controlled sites manner. Also drug infiltration through cell membranes is a modern challenge. Since Nano boron nitride has unique properties, it is one of the most promising mineral nanostructures ever explored. In this review, all the practical aspects of boron atoms in drug delivery and andnanostructured drugs are surveyed and the nano-boron nitride application is taken in review much more.

1. Introduction

In 2017, a mechanism for drug release based on low pH of cancerous tissues was proposed. According to DFT results, the protons can attack the region of interaction, separating the drug form the carrier. The interaction of 5-FU (5-fluorouracil anti-cancer drug) with pristine fullerene with absorption energy of about -3.2 kcal/mol, which is not suitable for drug delivery, is very poor. To overcome this problem one carbon atom is replaced by a boron atom that increases the adsorption energy to -27.2 kcal per mole.

B-doping sensitizes the electronic properties of fullerene to the drug [1] (Figure 1).

Also the electronic sensitivity of the pristine, Al, and Si doped BC₂N nanotubes toward CT drug was studied using DFT calculations. The CT drug prefers to be adsorbed on the all nanotubes via its -NH₂ group rather than O-head. The relative reactivity of the studied nanotubes toward the CT drug is as follows: Al-doped » Si-doped > Pristine, with adsorption energy about -48.8, -15.7, and -14.6 kcal/mol (Figure 2).

It was concluded that the Si-doped BC₂N nanotube may

be a promising candidate for application in CT sensors which benefits form a short recovery time, high sensitivity and selectivity [2].

Due to the rapid development of nanoscience in the production of new drugs, an attempt was made to review the application of boron nitride nanostructures (Figure 3) in the synthesis of effective drugs.

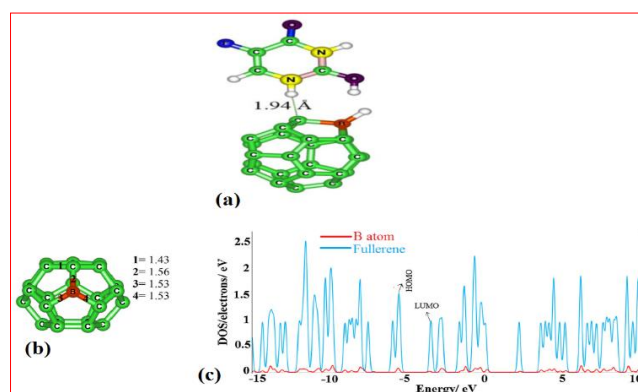


Figure 1. (a) The optimized structure of the 5-FU/B-C₂₄ complex which is assumed to be protonated in the low pH of the cancerous tissues, (b) Optimized structure of B-

* Corresponding author: e-mail: soma.majedi@uhd.edu.iq

doped C24 fullerene, (c) Partial density of states (DOS) plot of B-doped C24 fullerene.

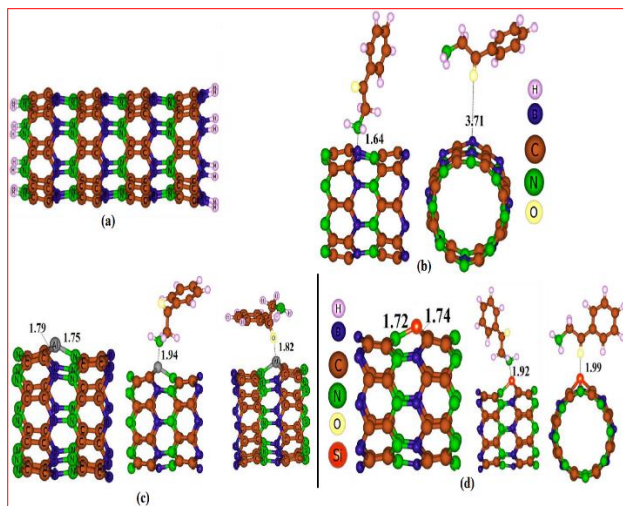


Figure 2. (a) Optimized structure of BC2N nanotube, (b) Optimized structures of CT/BC2N nanotube complexes. Distances are in Å, (c) Partial views of the optimized structures of Al-doped BC2N nanotube and its complexes with the CT drug. Distances are in Å, (d) Partial views of the optimized structures of Al-doped BC2N nanotube and its complexes with the CT drug. Distances are in Å.

Boron nitride with the chemical formula BN, is a thermal and chemical refractory compound of boron and nitrogen (Figure 4). It exists in various crystalline forms which as a carbon network are similarly structured isoelectric.

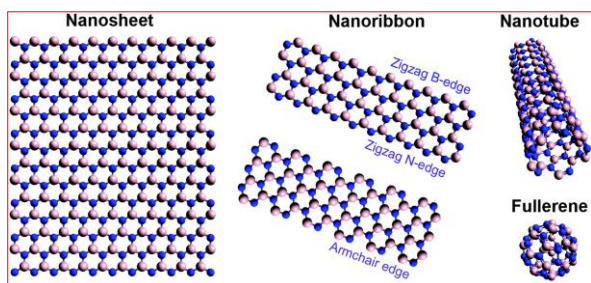


Figure 3. Nanostructures of boron nitride

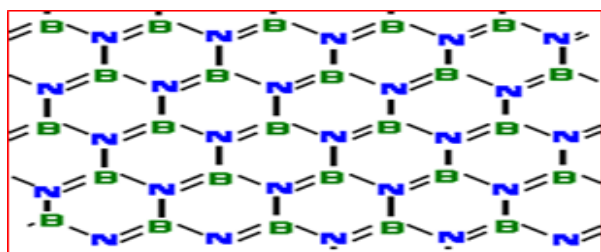


Figure 4. Section of a layer of hexagonal boron nitride (BN)

Significant attention has been paid to the research of boron nitride nanotubes due to their applications in futuristic electronic and mechanical devices. Boron nitride nanotubes are wide band gap semiconductors, chirality [3], have significant mechanical properties [4] and great thermal conductivity [5]. BNNTs are chemical stable and are used in high-temperature and hazardous

environments [6] (Figure 5). Nanoscale have been researched in lots of medical and biological usage namely anticancer therapy, bio-sensing technologies, biological separation and molecular imaging [7]. Boron nitride nanostructures have received widespread attention in the field of nanomedicine due to their inherent noncytotoxicity along with unique mechanical and electronic structural properties [8].

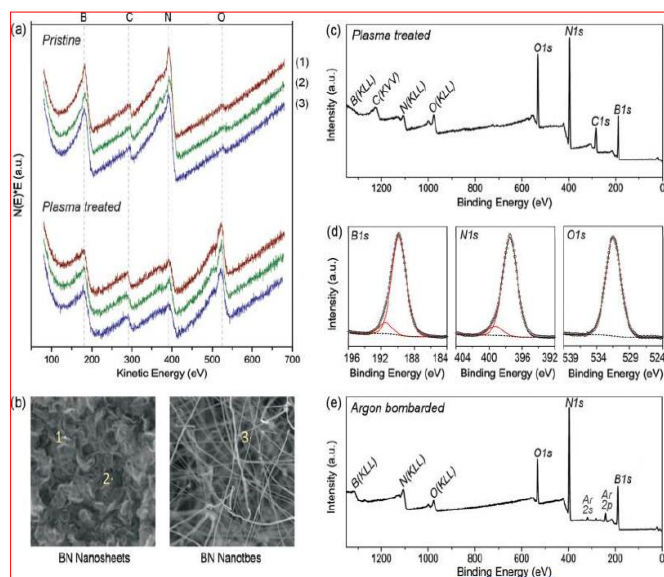


Figure 5. (a) AES spectra taken from the edges (1) and planes (2) of a BN nanosheet and walls of a BN nanotube (3) before and after air-plasma treatment; (b) SEM images of the BN nanostructures indicating the points from which the AES spectra were collected; (c) XPS survey spectrum of BN nanosheets after air-plasma treatment; (d) high-resolution core-level photoemission spectra of boron, nitrogen and oxygen; (e) XPS survey spectrum of BN nanosheets after air-plasma treatment and argon ion sputtering.

BN nanostructures are a zigzag (6, 0) BNNT, a BN sheet with 36 B and 36 N atoms, and a B₁₂N₁₂ nanocage. Dangling bonds of the nanotube and sheet are saturated with hydrogen atoms to reduce the edge effects on the results. The adsorption energy (E_{ad}) is obtained as follows [9]:

$$E_{ad} = E(BN) + E(cathinone) - E(cathinone/BN) + E(BSSE)$$

$E(BN)$ = Total energy of a BN nanostructure.

$E(cathinone/BN)$ = Total energy of the adsorbed cathinone molecule on the BN surface.

$E(BSSE)$ = The basis set superposition error (BSSE) which has been obtained using the counter poise method.

The interaction of cathinone drug with the B₁₂N₁₂ nanocage, a BNNT, and a BN sheet was calculated by using DFT [10]. Based on that the drugs adsorb on the B atom of the BN nanostructures. Adsorption energy for an example of a drug, for cage, tube, and sheet, was about 16.1, 14.0 and -5.0 kcal/mol, respectively. The electrical conductivity of a cathinone is increased when it is adsorbed on the BN nanostructures, therefore they can be employed in chemical sensors. The order of magnitude of the sensitivity:

$$S_{Cage} > S_{Tube} > S_{Sheet}$$

Sequence is in accordance with the decline of structural curvature of the BN nanostructures. Finally, a short recovery time of about 0.54 s, 0.02 s and 4.4 ns is predicted for cage, tube and sheet, respectively, at 298 K. The B₁₂N₁₂ structure benefits from a high sensitivity (46.0% change of E_g upon the drug adsorption), short recovery time, and no need to structural manipulation [10]. The B₁₂N₁₂ nanocage is consisted from 8 hexagonal and 6 tetragonal rings with 36 B-N bonds. These bonds are two type, namely, [4,6]- and [6,6]- bonds with average length of 1.48, and 1.43 Å, respectively. The [4,6]-bonds are shared by a four- and a six-membered ring and [6,6]- bonds between two six-membered rings. The [4,6]-bonds are shorter due to the higher strain in the tetragonal rings compared to the hexagons. The DOS plot (Figure 4) and the results in Table 1 indicate that the energies of HOMO and LUMO levels are about -7.70 and -0.86 eV, respectively. Thus, the E_g is about 6.84 eV. HOMO and LUMO levels are mainly located on the N and B atoms, respectively and the energies of HOMO and LUMO levels of BNNT are about -6.26 and -1.96 eV, respectively. HOMO level is mainly located on the N atoms which is closed to the N head of the tube and the LUMO is mainly located on the B atoms on the opposite site. (Figure 4) [10].

Structure	E_{ad}	E_{HOMO}	E_{LUMO}	E_g	$\% \Delta E_g$	Q (e)
Cage	-	-7.70	-0.86	6.84	-	-
Tube	-	-6.26	-1.96	4.30	-	-
Sheet	-	-6.30	-0.42	5.88	-	-
Cage-O	-5.8	-6.28	-3.34	2.94	-57.0	0.25
Tube-O	-2.6	-5.97	-2.86	3.11	-27.6	0.15
Sheet-O	-0.5	-6.22	-1.66	4.56	-23.0	0.03
Cage-N	-16.1	-6.29	-2.60	3.69	-46.0	0.33
Tube-N	-14.0	-6.02	-2.39	3.63	-15.5	0.24
Sheet-N	-5.0	-6.13	-1.01	4.84	-12.9	0.09

Table 1. Energy of HOMO, LUMO, HOMO-LUMO gap (E_g) in eV, and the change of E_g upon the drug adsorption on the BN nanostructures. The adsorption energy (E_{ad}) is in kcal/mol. Q is the NBO charge transfer from the drug to the BN nanostructures. All calculations were performed at B3LYP-D/6-31G*.

The cathinone has two nucleophile sites including amine (N-head) and carbonyl (O-head) groups which can attack to the electrophile sites (B atoms) of the BN nanostructures (Figure 4). Thus, the optimized structures of two drug/BN complexes are shown in Figure 4 in which the drug is adsorbed from its O- or N-head on a B atom of BN cage. Afterward we name the complexes as O-cage or N-cage. In the O-cage, the newly formed O-B bond length is about 1.57 Å and also an interaction with the H atoms of drug and the N atom of the cage can be seen in a distance of 2.15 Å (Figure 4). The calculated adsorption energy is about -5.8 kcal/mol. The small distance between O and B (~1.57 Å) indicates that the interaction may be strong and thus the small adsorption energy (less negative) may be due to the deformation of the structure of the cage. After the adsorption process the adsorbing B

atom is projected out and the N-B-N angle of tetragon is decreased from 96° to 84° and also the [4,6]- bond is increased from 1.48 to 1.58 Å. In the N-cage, the newly formed N-B bond length is about 1.61 Å, and also, an interaction with the H atoms of drug and the N atom of the cage is predicted at a distance of 2.70 Å. The calculated adsorption energy for N-cage is about -16.1 kcal/mol. After the adsorption process the adsorbing B atom is somewhat projected out and the corresponding N-B-N angles are decreased. The adsorption energies demonstrate that adsorption of the drug from its N-head is much stronger than that from the O-head. The frontier molecular analysis indicates that the HOMO level is located on both N and O atoms of the drug but the LUMO on the whole molecule except -NH₂ group. Locating the LUMO on the O-head weakens the interaction of O-head with the electron deficient B sites. Also, the -NH₂ group is more accessible compared to the -O- site because of steric hindrance (Figure 6) [10].

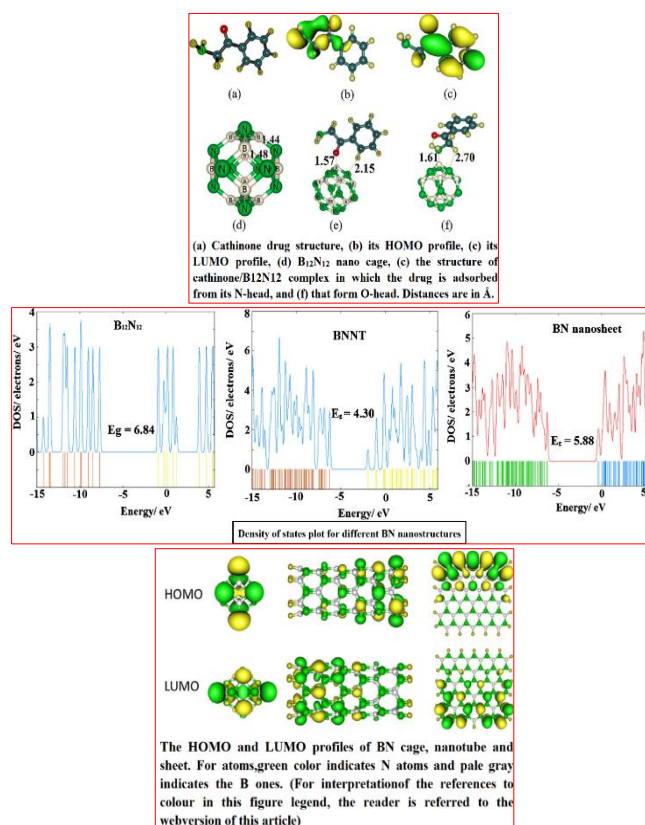


Figure 6. The optimized structures of the BN nanostructures

By performing density functional theory calculations, the using of a synthesized boron nitride nanocluster (B₁₂N₁₂) as a potential chemical sensor for anticancer α -cyano-4-hydroxycinnamic acid (CHC) drug was inspected [11]. It was found that the drug prefers to be adsorbed from its -COOH group on a hexagon of the BN cluster with adsorption energy about -23.7 kcal/mol. After the adsorption of the CHC drug, the LUMO level of BN nanocluster meaningfully stabilizes so that the E_g is largely decreased. So, the BN nanocluster converts to

a semiconductor with higher electrical conductivity. The increase of electrical conductivity can generate an electrical signal which helps to detect the CHC drug. By increasing the %HF exchange of the functional, the adsorption energy and sensitivity are increased and decreased, respectively. The sensitivity of the BN nanocluster decrease in water solution (Figure 7).

Tabun, the extremely toxic chemical substance, a colorless and tasteless species with a faint fruity odor, is classified as a strong nerve agent because this compound extremely interferes with normal functioning of the mammalian nervous system [12].

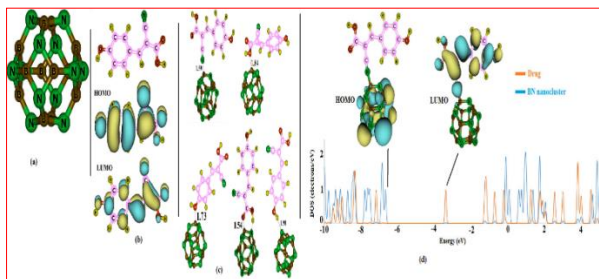


Figure 7. (a) Optimized structure (b) Optimized structure, HOMO and LUMO profiles of CHC drug (complex A) (c) Optimized structures of the CHC/B₁₂N₁₂ nanocluster complexes. Distance is in Å. (d) Partial density of states of complex A, and its HOMO and LUMO profiles

Boron or a nitrogen atom doping on the fullerene C₂₀, leads to the step-by-step adsorption process of the Tabun [13]. The results show that the adsorption mechanism of Tabun 2D-skeletal (Tabun nerve agent) proceeds via a multistep pathway, in each considered case (Figure 8). For C₂₀ fullerene, the first step adsorption energy which leads to C₂₀-T geometry is about -1.00 kcal mol⁻¹; while, the second step adsorption energy, is about -1.27 kcal mol⁻¹ which belongs to C₂₀-T₁ orientation. Further input files for the decomposition of Tabun on the surface of C₂₀ fullerene did not optimized truly; while, in other cases (C₁₉N, and C₁₉B), the adsorption of Tabun gas, led to destruction of that species (C₁₉N-T₁, and C₁₉B-T₂). The first adsorption step of Tabun on the surface of C₁₉N leading to emergence of C₁₉N-T, was about -1.68 kcal mol⁻¹, and the second step adsorption of it, led to emergence of C₁₉N-T₁ (25.4 kcal mol⁻¹, decomposition of Tabun). The high energy difference between C₁₉N-T, and C₁₉N-T₁ (23.7 kcal mol⁻¹) showed that the decomposition process of Tabun on the surface of C₁₉N fullerene occurs so fast. The same results were produced for C₁₉B fullerene.

The effect of Hartree-Fock (HF) exchange percentage of a density functional on the adsorption properties and electronic sensitivity of the B₁₂N₁₂ nanocluster to CO molecule was studied in 2016 [14]. It was found that functionals with more than 30% HF exchange fail to properly predict the HOMO, E_g, E_{ads} and bond length. A parabolic relation between E_{ads} and %HF exchange is obtained. Although at all levels of theory the B₁₂N₁₂

shows an electronic sensitivity toward CO molecule, it is slightly increased by an increase in the %HF. The functionals with a large %HF such as (M06-HF (100%), M06-2X (54%), ect) may significantly overestimate the E_g, and bond strength.

By substituting a carbon atom by a boron atom, the geometric structure of phagraphene, as a carrier for adrucil drug, is somewhat distorted [15].

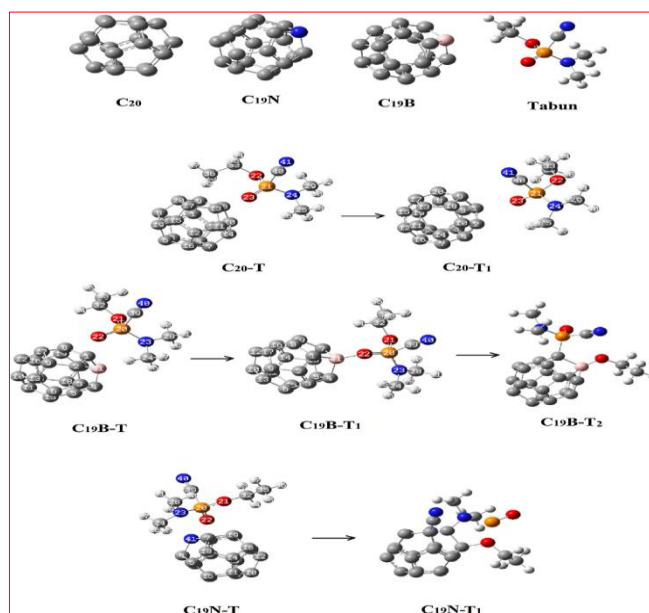


Figure 8. The adsorption steps of Tabun nerve agent by using C₂₀ fullerene and its derivatives, optimized at B3LYP/6-311G (d,p) level.

In 2015, phagraphene was introduced as a novel nanostructure [16]. The calculated B-C bond lengths are about 1.48, 1.49 and 1.54 Å which are longer than the corresponding C-C bonds in the pristine phagraphene. In addition, the C-B-C angle of pentagon is about 105.9° which is smaller than the corresponding angle in the pristine phagraphene (130.3°). This indicates that the B atom is projected out of the surface. The results of Tables 1 and 2 demonstrate that the HOMO, LUMO, and E_g of the phagraphene are significantly changed after the B-doping process. The energies of HOMO and LUMO of the B-doped phagraphene are about -4.40 and -3.57 eV, respectively, which produce an E_g about 0.83 eV. This indicates that the B-doping stabilizes the HOMO and destabilizes the LUMO of phagraphene which leads to a gap opening by about 0.35 eV (Figure 9).

Over the past decades, development of effective drug delivery systems has attracted considerable attention, because of their potential to deliver high concentrations of drugs to a target tissue [17-18]. Nevertheless, many of these drug delivery systems suffer from numerous limitations in terms of toxicity, immunogenicity, cost, and safety issues. However, there are numerous evidences that indicate the pharmacological properties of conventional drugs can be improved along the usage of nanocarriers [19-20].

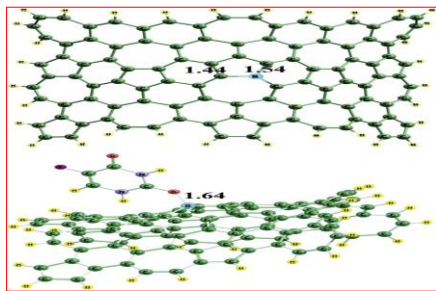


Figure 9. Optimized structure of B-doped phagraphene and its complex with adrucil. Distances are in Å.

These nanocarriers combine with the different drugs and target issue receptors except some inconvenient [21-22]. Generally speaking, an ideal drug delivery process has three following steps: first, the drug is attached to the surface of nanocarrier; then, it is transferred to the target tissue and finally the drug is released. The outstanding characteristics of boron nitride (BN) nanostructures can improve the attachment of drugs over them [23-26].

The interaction of an aspirin (AS) molecule with the external surface of a boron nitride fullerene-like nanocage ($B_{12}N_{12}$) is studied by means of density functional theory (DFT) calculations [27]. The results clearly indicate that Al-doping of the $B_{12}N_{12}$ tends to increase the adsorption energy and thermodynamic stability of AS molecule over this nanocage. By further study about the adsorption of AS over the $B_{12}N_{12}$ and $B_{11}N_{12}Al$ in the presence of a protic (water) or aprotic (benzene) solvent, it was found that the calculated binding distances and adsorption energies by the PCM (polarizable continuum model) and CPCM (conductor-like polarizable continuum model) solvent models are very similar, especially for the $B_{12}N_{12}$ complexes. AS molecule is strongly adsorbed over the $B_{12}N_{12}$ and $B_{11}N_{12}Al$ nanocages in the gas phase due to the large negative E_{ads} , ΔG_{298} , and ΔH_{298} values. As a result, these nanocages can act as a potentially sensor for AS detection. Both $B_{12}N_{12}$ and $B_{11}N_{12}Al$ nanocages can act as an appropriate substrate for the adsorption of AS molecule in the protic and aprotic solvents (Figure 10) (Table 2, Table 3).

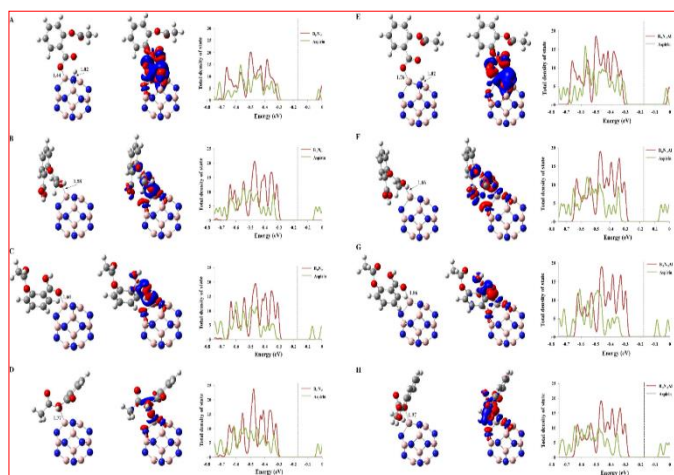


Figure 10. Optimized structures of adsorbed aspirin over the $B_{12}N_{12}$ nanocage (left) along with their corresponding EDD maps (0.001 au) (middle) and PDOS plots. In the EDD maps, the electron density depletion and accumulation sites are displayed in red and blue, respectively. All bond distances are in Å. In the PDOS plots, the dashed line indicates Fermi level.

Table 2. Calculated binding distances (R, Å), adsorption energy (E_{ads} , kcal/mol), NBO charge-transfer (q_{CT} , e), change in Gibbs free energy (ΔG_{298} , kcal/mol), change in enthalpy (ΔH_{298} , kcal/mol), HOMO–LUMO energy gap (E_g , eV), and dipole moment (μ , Debye) of adsorbed aspirin over $B_{12}N_{12}$ and $B_{11}N_{12}Al$ nanocages in benzene phase

Configuration	R	E_{ads}	q_{CT}	ΔG_{298}	ΔH_{298}	E_g	μ
$B_{12}N_{12}$							
A	1.44 (1.45)	-37.0 (-33.6)	0.01 (0.01)	-23.4 (-20.8)	-36.0 (-32.5)	7.8 (3.8)	3.53 (3.41)
B	1.57 (1.60)	-23.6 (-20.3)	-0.31 (-0.31)	-8.1 (-4.7)	-22.5 (-18.2)	7.4 (3.2)	10.56 (10.81)
C	1.58 (1.61)	-18.7 (-17.6)	-0.32 (-0.31)	-5.9 (-2.4)	-17.5 (-16.1)	6.7 (2.5)	9.60 (9.37)
D	1.74 (2.24)	-9.7 (-9.6)	-0.23 (-0.10)	4.4 (5.8)	-8.7 (-8.5)	7.9 (4.2)	4.89 (2.14)
$B_{11}N_{12}Al$							
E	1.76 (1.78)	-72.9 (-68.0)	0.22 (0.22)	-59.1 (-54.6)	-71.7 (-66.4)	7.7 (3.8)	4.82 (4.68)
F	1.84 (1.87)	-53.4 (-49.2)	-0.15 (-0.11)	-38.6 (-34.5)	-52.1 (-47.8)	6.9 (2.7)	13.95 (13.76)
G	1.84 (1.87)	-49.0 (-46.0)	-0.17 (-0.17)	-35.4 (-32.0)	-47.4 (-44.1)	6.0 (2.2)	14.56 (14.06)
H	1.96 (2.01)	-42.4 (-40.3)	-0.22 (-0.21)	-29.7 (-27.8)	-41.6 (-38.4)	6.5 (2.5)	11.11 (11.56)

The values out of the parenthesis refer to the M06-2X/6-31 + G** method, while the calculated values by the M06-2X/6-31 + G** method are given within the parenthesis. The negative value of q_{CH} indicates the electron density transfer from AS molecule to the $B_{12}N_{12}$ or $B_{11}N_{12}Al$ surface.

Table 3. Calculated maximum absorption wavelength (λ_{max}), corresponding oscillator strength (f) and main orbital interaction of the AS- $B_{12}N_{12}$ and AS- $B_{11}N_{12}Al$ complexes at the M06-2X/6-31 + G** level

Phase	Complex	f	λ_{max} (nm)	Assignment
Gas	A	0.261	180	HOMO → LUMO (33.9 %)
	B	0.287	198	HOMO-4 → LUMO + 1 (18.3 %)
	C	0.272	181	HOMO → LUMO + 1 (45.5 %)
	D	0.189	231	HOMO-7 → LUMO (40.6 %)
	E	0.407	186	HOMO → LUMO (36.4 %)
	F	0.258	201	HOMO-8 → LUMO (28.3 %)
	G	0.124	215	HOMO-3 → LUMO + 1 (46.5 %)
	H	0.091	236	HOMO-10 → LUMO (40.6 %)
Water	A	0.452	183	HOMO → LUMO (50.8 %)
	B	0.491	202	HOMO-4 → LUMO (27.5 %)
	C	0.335	180	HOMO-1 → LUMO + 1 (17.6 %)
	D	0.287	181	HOMO-2 → LUMO + 1 (44.8 %)
	E	0.476	185	HOMO → LUMO (49.2 %)
	F	0.237	202	HOMO-4 → LUMO (34.5 %)
	G	0.231	186	HOMO-3 → LUMO + 1 (19.5 %)
	H	0.134	242	HOMO-2 → LUMO (42.8 %)
Benzene	A	0.460	186	HOMO → LUMO (48.6 %)
	B	0.540	187	HOMO-3 → LUMO + 1 (42.9 %)
	C	0.394	184	HOMO → LUMO + 1 (21.6 %)
	D	0.210	238	HOMO-6 → LUMO (42.6 %)
	E	0.577	188	HOMO → LUMO (54.2 %)
	F	0.326	205	HOMO-3 → LUMO + 1 (36.1 %)
	G	0.411	189	HOMO-7 → LUMO + 1 (28.8 %)
	H	0.276	242	HOMO-9 → LUMO (87.8 %)

References:

- [1] A. Hosseini, E. Vessally, S. Yahyaei, L. Edjlali, A. Bekhradnia, *J. Clust. Sci.* 28 (2017) 2681–2692.
- [2] K. Nejati, E. Vessally, P. Delir Kheirollahi Nezhad, H. Mofid, A. Bekhradnia, *J. Phys. Chem. Solids*, 111 (2017) 238–244.
- [3] (a) Blase, X.; Rubio, A.; Louie, S. G.; Cohen, M. L. *Europhys. Lett.* 1994, 28, 335. (b) Rubio, A.; Corkill, J. L.; Cohen, M. L. *Phys. Rev. B* 1994, 49, 5081.
- [4] Chopra, N. G.; Zettl, A. *Solid State Commun.* 1998, 105, 297, (b) A. Pakdel, Y. Bando, D. Golberg, *Chem. Soc. Rev.* 43 (2014) 934–959.
- [5] (a) Xiao, Y.; Yan, X. H.; Cao, J. X.; Ding, J. W.; Mao, Y. L.; Xiang, J. *Phys. Rev. B* 2004, 69, 205415, (b) Han, W. Q.; Mickelson, W.; Cumings, J.; Zettl, A. *Appl. Phys. Lett.* 2002, 81, 1110, (c) A. Pakdel, C.Y. Zhi, Y. Bando, D. Golberg, *Mater. Today* 15 (2012) 256–265.
- [6] Golberg, D.; Bando, Y.; Kurashima, K.; Sato, T. *Scripta Materialia* 2001, 44, 1561.
- [7] (a) A. Star, E. Tu, J. Niemann, J. C. P. Gabriel, C. S. Joiner and C. Valcke, *Proc. Natl. Acad. Sci. USA*, 2006, 103, 921–926, (b) SS Wong, E Joselevich, AT Woolley, CL Cheung, CM Lieber. *Nature* 394 (1998), 52-55, (c) X Chen, A Kis, A Zettl, CR Bertozzi. *Proceedings of the National Academy of Sciences* 104 (2007), 8218-8222, (d) K. Kostarelos, L. Lacerda, G. Pastorin, W. Wu, S. Wieckowski, J. Luangsivilay, S. Godefroy, D. Pantarotto, J. Briand, S. Muller, M. Prato, A. Bianco, *Nat Nanotechnol.* 2 (2007) 108-113, (e) N.W. S. Kam, M. O' Connell, J. A. Wisdom, H. Dai. *Proc. Natl Acad. Sci. USA* 102, (2005) 11600-11605.
- [8] (a) X. Chen, P. Wu, M. Rousseas, D. Okawa, Z. Gartner, A. Zettl, C. R. Bertozzi, *J Am Chem Soc.* 131, 3 (2009) 890-891, (b) G Ciofani, S Danti, D D'Alessandro, S Moscato, A Menciassi. *Biochemical and biophysical research communications* 394 (2010), 405-411, (c) G. Ciofani, *Expert Opin. Drug Deliv.* 7 (2010) 889–893, (d) G. Ciofani, S. Danti, L. Ricotti, D. D'Alessandro, S. Moscato, V. Mattoli, and A. Menciassi, *Current Nanoscience* 7 (1), 94-109, (e) G. Ciofani, S. Danti, G.G. Genchi, D. D'Alessandro, J.L. Pellequer, M. Odorico, V. Mattoli, M. Giorgi, *Int. J. Nanomedicine* 7 (2012) 19-24, (f) G. Ciofani, S. Danti, *Methods Mol Biol.* 811 (2012) 193-206.
- [9] S.F. Boys, F. Bernardi, Calculation of small molecular interactions by differences of separate total energies – some procedures with reduced errors, *Mol. Phys.* 19 (1970) 553–561.
- [10] K. Nejati, A. Hosseini, E. Vessally, A. Bekhradnia, L. Edjlali, *Appl. Surf. Sci.* 422 (2017) 763–768.
- [11] A. Hosseini, E. Vessally, A. Bekhradnia, S. Ahmadi, P. Delir Kheirollahi Nezhad, *J. INORG. ORGANOMET. P.* 28 (2018) 1422–1431.
- [12] (a) L. Larsson, *Acta. Chim. Scand.* 12 (1958) 783–785, (b) B. Simpson, *Biotechnol. J.* 2 (2004) 100–105.
- [13] S. A. Siadatia, E. Vessally, A. Hosseini, L. Edjlali, *Synthetic Metals* 220 (2016) 606–611.
- [14] E. Vessally, S. Soleimani-Amiri, A. Hosseini, L. Edjlali, A. Bekhradnia, *Physica E* 87, 308–311.
- [15] R. Bagheri, M. Babazadeh, E. Vessally, M. Es'haghi, A. Bekhradnia, *Inorg. Chem. Commun.* 90 (2018) 8–14.
- [16] Z. Wang, X.-F. Zhou, X. Zhang, Q. Zhu, H. Dong, M. Zhao, A.R. Oganov, *Nano Lett.* 15 (2015) 6182–6186.
- [17] J. Kreuter (1994) *Colloidal drug delivery systems*. CRC Press, New York.
- [18] K.S. Soppimath, T.M. Aminabhavi, A.R. Kulkarni, W.E. Rudzinski, *J. Control Release* 70 (2001) 1–20.
- [19] D. Peer, J.M. Karp, S. Hong, O.C. Farokhzad, R. Margalit, R. Langer, *Nat Nanotechnol* 2 (2007) 751-760.
- [20] V.P. Torchilin, *Pharm Res* 24 (2007) 1–16.
- [21] L.S. Jabr-Milane, L.E. van Vlerken, S. Yadav, M.M. Amiji, *Cancer Treat Rev*, 34 (2008) 592–602.
- [22] L.E. van Vlerken, M.M. Amiji, *Expert Opin Drug Deliv* 3 (2006) 205–216.
- [23] E. Duverger, T. Gharbi, E. Delabrousse, F. Picaud, *Phys Chem Chem Phys* 16 (2014) 18425–18432.
- [24] D. Farmanzadeh, S. Ghazanfary, *C R Chim* 17 (2014) 985–993.
- [25] N. Saikia, S.K. Pati, R.C. Deka, *Appl Nanosci* 2 (2012) 389–400.
- [26] M.T. Baei, M.R. Taghartapeh, E.T. Lemeski, A. Soltani, *Phys B* 444 (2014) 6–13.
- [27] E. Vessally, M.D. Esrafil, R. Nurazar, P. Nematollahi, A. Bekhradnia, *Struct. Chem.* 28 (2017) 735–74

How to Cite This Article

Majedi, S., Farnaz Behmagham, and M. Vakili. "Theoretical view on interaction between boron nitride nanostructures and some drugs." *J. Chem. Lett* 1 (2020): 19-24.